WEP Warwick Evans Publishing

International Journal of Materials Science and Technology Studies

ISSN: 3006-7693 (Print), ISSN: 3006-3744 (Online) | Volume 3, Number 2, Year 2025
DOI: https://doi.org/10.62051/ijmsts.v3n2.07
Journal homepage: https://wepub.org/index.php/IJMSTS/index

Microstructural Characteristics and Tribological Properties of Graphene-Reinforced Magnesium Matrix Composites Fabricated via Rotary Friction Extrusion

Tengfei Du, Tian Yan

School of Nanchang Hangkong University, NanChang 330063, China

ABSTRACT

The Rotational Friction Extrusion (RFE) technique was successfully employed to fabricate graphite particle-reinforced AZ31 magnesium matrix composites (Gr/AZ31Mg). The microstructure, hardness, and wear properties of the composites were systematically analyzed. The results indicate that the RFE process enables the production of rod-shaped Gr/AZ31Mg composites with well-defined dimensions and high forming quality. The microstructure of the composites consists of fine equiaxed grains formed through dynamic recrystallization, with uniformly distributed Gr particles within the magnesium matrix, contributing to enhanced overall performance. Hardness measurements reveal that the addition of Gr significantly influences the hardness of the composites, exhibiting an initial increase followed by a slight decline. When the Gr content reaches 1.5 wt.%, the composite's hardness is improved by 20.2% compared to the unreinforced AZ31Mg matrix. Regarding wear performance, Gr particles act as solid lubricants during the friction process, reducing direct contact wear, thereby decreasing wear volume and enhancing wear resistance. The variation trends of the friction coefficient and wear rate align with those of hardness; both parameters initially decrease with increasing Gr content and then exhibit a slight rebound. At a Gr content of 1.5 wt.%, the composite achieves the lowest wear rate of 0.197, representing a 33.7% reduction compared to the RFE-processed AZ31Mg matrix, indicating optimal wear resistance at this reinforcement level.

KEYWORDS

Rotational Friction Extrusion; Composite Materials; Microstructure; Wear Performance

1. INTRODUCTION

Magnesium alloys have garnered significant attention for structural applications in the automotive and aerospace industries due to their exceptional thermal conductivity, high specific strength, favorable stiffness, and damping characteristics, coupled with excellent machinability and recyclability [1-7]. Notably, performance-optimized magnesium-based composites have demonstrated remarkable enhancements in mechanical properties, laying a solid foundation for their utilization in high-performance structural materials. Nevertheless, despite these advantages, inherent limitations such as low elastic modulus, restricted plasticity, and inferior corrosion resistance continue to impede their widespread adoption in critical engineering applications [5-9]. In response to these challenges, recent research efforts have focused on refining the comprehensive properties of magnesium alloys through strategies including alloying, surface modification, and composite design, thereby expanding their potential engineering applications.

One-dimensional carbon nanotubes (CNTs) and two-dimensional graphene nanosheets (GNS) are widely regarded as ideal candidates for reinforcing metal matrix composites (MMCs) due to their exceptional mechanical, electrical, and thermal properties. Compared to traditional ceramic or

metallic particle reinforcements, carbon-based nanofillers not only exhibit lower density but also significantly enhance the specific strength and stiffness of composites, offering unique advantages in the field of high-performance lightweight structural materials. Furthermore, CNTs and GNS demonstrate ultrahigh Young's modulus, superior hardness, and excellent compressive and flexural strength, along with remarkable thermal stability, enabling them to maintain structural integrity and performance even under extreme conditions. Notably, the high modulus of nanocarbon materials facilitates effective second-phase strengthening mechanisms, further optimizing the overall mechanical properties of the composites.

Saikrishna et al. [10] employed friction stir processing (FSP) to fabricate multi-walled carbon nanotube (MWCNT)-reinforced metal matrix composites (MMCs) and evaluated their microhardness. The results demonstrated that the incorporation of MWCNTs significantly enhanced the microhardness of the composites, exhibiting superior mechanical properties compared to pure magnesium. Additionally, electrochemical tests revealed that the introduction of MWCNTs effectively improved the corrosion resistance of the composites, highlighting their potential for anti-corrosion applications.

Kandemir et al. [11] utilized high-shear dispersion technology to produce recycled short carbon fiber-reinforced composites and systematically investigated their mechanical properties. Vickers hardness (HV) tests indicated that the hardness of the composites increased by 6.5% and 13% for carbon fiber lengths of 100 μm and 500 μm, respectively, compared to the matrix material. Further experiments demonstrated that the addition of short carbon fibers not only significantly enhanced the compressive strength of the composites but also maintained high mechanical strength without increasing the minimum creep rate, suggesting promising applications in high-temperature structural materials.

Meng et al. [12] fabricated graphene nanoplatelet (GNP)-reinforced magnesium-based laminated metal matrix composites (LMMCs) through hot-press sintering and rolling processes. The results showed that at a GNP volume fraction of 0.25 vol.%, the tensile strength of the composite reached 160 MPa, lower than that of the 0.75 vol.% GNP composite (179 MPa) but significantly higher than that of pure magnesium (136 MPa). Microstructural analysis revealed that the incorporation of GNPs effectively inhibited crack propagation while maintaining the ductility of the composites, thereby balancing strength and toughness. This makes GNPs-reinforced composites highly promising for lightweight, high-strength structural applications.

Rotational friction extrusion (RFE), a solid-state material processing technique derived from the principles of friction stir processing (FSP), was employed in this study. Our research team has optimized the RFE process based on FSP, utilizing frictional heating and plastic deformation to achieve homogeneous material mixing, thereby producing bulk composites with fine grains, uniform microstructures, and excellent mechanical properties. RFE offers several advantages, including high material utilization efficiency, simplified processing steps, and the ability to fabricate bulk composites with varying cross-sectional dimensions, making it a promising method for manufacturing high-performance metal matrix composites.

In this study, RFE was utilized to fabricate graphene-reinforced AZ31 magnesium matrix composites (Gr/AZ31Mg), and their microstructure, hardness, and wear properties were systematically investigated to elucidate the influence of this method on the microstructural evolution and mechanical performance of the composites.

2. EXPERIMENTAL MATERIALS AND METHODS

The rotational friction extrusion (RFE) experiments utilized AZ31 magnesium alloy plates as the base material, with their elemental composition detailed in Table 1. The plates were sectioned into strip-shaped specimens measuring 100 mm × 16 mm × 16 mm, and their surfaces were thoroughly polished

using abrasive paper to ensure optimal cleanliness. The mechanical and physical properties of the AZ31 magnesium alloy are presented in Table 2.

Table 1. Chemical Composition of AZ31 Magnesium Alloy

Element	Mg	Zn	Mn	Fe	Si	Al
wt.%	Bal.	0.92	0.28	0.031	0.027	3.05

Table 2. Mechanical and Physical Properties of AZ31 Magnesium Alloy

Material	Tensile Strength (MPa)	Yield Strength (MPa)	Elongation (%)	Hardness (HV)
AZ31 Magnesium Alloy	263	123	29	62

The reinforcing phase consisted of graphite (referred to as Gr) particles supplied by Guangzhou Baiyang Technology Co., Ltd. The particle size distribution ranged from 20 μm to 40 μm, with an average particle size of 30 μm. Figure 1 illustrates the morphological characteristics of the Gr particles.

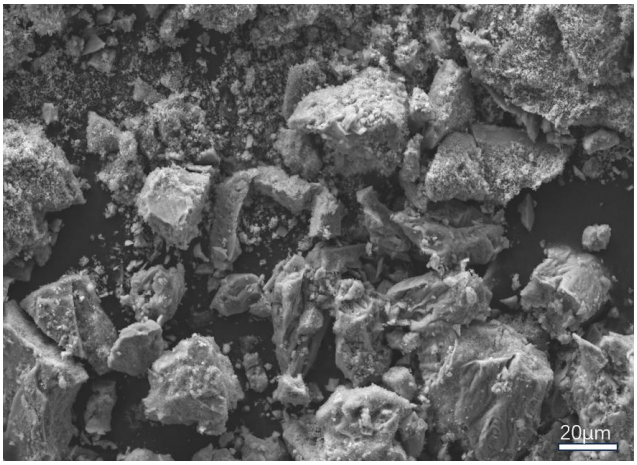

Figure 1. Morphology of Graphite (Gr) Particles

This study employed rotary friction extrusion (RFE) technology to fabricate graphite-reinforced magnesium matrix composites. Figure 2 illustrates the pre-processing schematic of the base material for RFE-based composite fabrication. The specific preparation procedure is as follows: First, eight blind holes with a diameter of 6 mm and a depth of 12 mm were machined along the central axis of the AZ31 magnesium alloy bar at intervals of 12 mm. Subsequently, the holed specimens were placed in an ultrasonic cleaning system and sequentially cleaned with anhydrous ethanol and deionized water to effectively remove residual machining oil and metal debris from the surfaces and holes. After cleaning, precisely weighed graphite powder was uniformly distributed into the holes using a compaction filling process, ensuring the graphite mass fraction was accurately controlled within the range of 0.5% to 2%. For clarity, this work defines the following terms: the unmodified original AZ31 magnesium alloy is referred to as the AZ31 base material; the magnesium alloy processed by RFE without reinforcement is termed the RFE-processed base material; and the composite system containing 1 wt.% graphite is labeled as the 1%Gr/AZ31Mg composite.

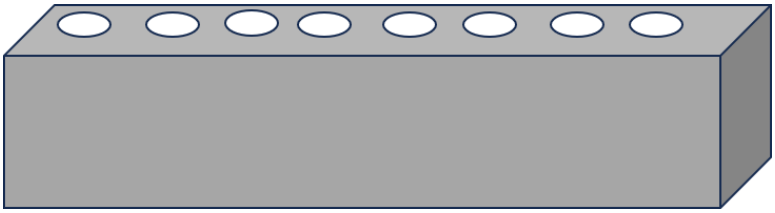

Figure 2. Schematic of Base Material Pre-Processing for RFE Fabrication

This figure 3 depicts the schematic of the rotary friction extrusion (RFE) processing setup, which operates based on the thermo-mechanical coupling principle. The pre-processed specimen is placed in a custom-designed extrusion mold cavity and constrained axially using a pressure plate. Under the action of the drive system, the high-speed rotating tool head, operating at 405 rpm, generates frictional heat at the contact surface with the specimen. When the local temperature reaches the critical value for plastic deformation of the magnesium alloy, the synergistic effects of mechanical force from the tool head and thermal activation enable the plasticized metal to flow through the mold outlet, achieving directional extrusion forming.

The entire process is controlled by a closed-loop system, with the extrusion head advancing at a precise rate of 0.25 mm/min to ensure stable material flow behavior and microstructural evolution. This process leverages the multi-field coupling effects of frictional heat, mechanical force, and material rheology to achieve gradient compositing and interface optimization between the reinforcing phase and the matrix.

Figure 3. Schematic of the RFE Processing Setup

3. RESULTS AND DISCUSSION

3.1. Composite Forming and Microstructure

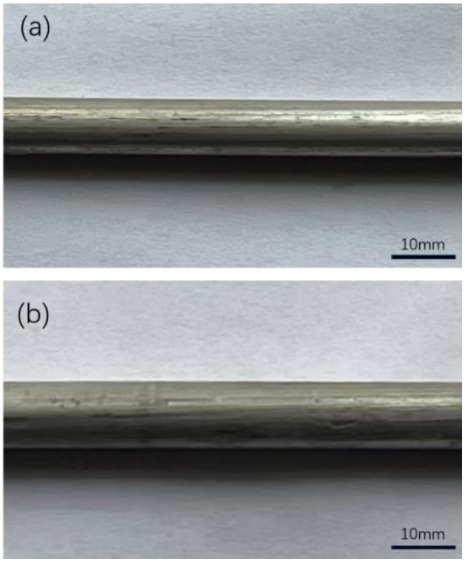

Figure 4. Surface Morphology of Materials Processed by RFE: (a) Base Material, (b) Gr/AZ31Mg Composite

Using rotary friction extrusion (RFE), rod-shaped Gr/AZ31Mg composites with a diameter of 6 mm and a length of 340 mm were successfully fabricated. Figure 4 shows the surface morphology of both the RFE-processed base material and the composite containing 1 wt.% graphite. As illustrated in the figure, the rods exhibit smooth surfaces, uniform dimensions, and no visible defects, highlighting the capability of the RFE process to produce high-quality composite materials with excellent surface integrity.

Figure 5(a) shows the microstructure of the unprocessed AZ31Mg base material, which consists of irregularly shaped grains with varying sizes. In contrast, Figure 5(b) presents the microstructure of the AZ31Mg composite reinforced with 1 wt.% graphite (Gr). The composite exhibits a refined microstructure composed of equiaxed grains, with significantly reduced grain sizes compared to the base material. However, some agglomeration of Gr particles is observed in the composite.

The notable grain refinement observed in this study is attributed to the multi-scale synergistic mechanisms during the rotary friction extrusion (RFE) process, which can be explained by the following two aspects:

Friction Heat-Shear Strain Coupling Effect:

Under the combined loading conditions of high-speed rotation (405 rpm) and axial extrusion (0.25 mm/min), the specimen undergoes high strain rate plastic deformation ($\sim 10^3\ s^{-1}$). Intense mechanical shear leads to an exponential increase in dislocation density, while frictional heating at the interface raises the local temperature to the critical value for dynamic recrystallization ($T \approx 0.6Tm$). These factors collectively promote continuous dynamic recrystallization (CDRX), transforming the original coarse grains (initial size > 50 μm) into submicron-sized equiaxed grains (average grain size < 2 μm) through a gradual decomposition mechanism.

Zener Pinning Effect of Second-Phase Particles:

The graphite (Gr) reinforcing phase is uniformly distributed along grain boundaries during plastic flow. Its high modulus ($E \approx 1$ TPa) significantly enhances the pinning efficiency. By establishing a critical resistance model for grain boundary migration: $\Delta P = 3f\gamma/(2r)$ (where f is the volume fraction of particles, γ is the grain boundary energy, and r is the particle radius), calculations indicate that Gr particles can generate a pinning force > 0.5 MPa, effectively inhibiting grain boundary migration and preventing abnormal grain growth.

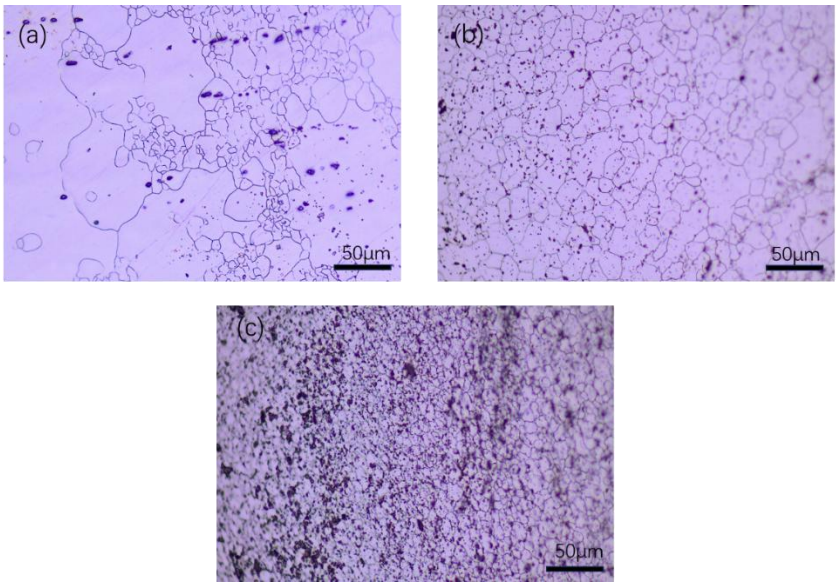

Figure 5. Metallographic Microstructure of Composites: (a) Base Material, (b) 1%Gr/AZ31Mg Composite, (c) 2%Gr/AZ31Mg Composite

3.2. Microhardness of Composites

Figure 6 illustrates the relationship between the hardness of Gr/AZ31Mg composites and the mass fraction of Gr. The dashed line represents the hardness of the base material (AZ31Mg), which is 62.0 HV. After RFE processing, the hardness of the RFE-processed base material increased to 68.5 HV, a 10.5% improvement over the base material. As shown in the figure, the hardness of the composites initially increases and then decreases with increasing Gr content. When the Gr content reaches 1.5 wt.%, the composite achieves its maximum hardness of 74.5 HV, representing a 20.2% increase compared to the base material. At 2 wt.% Gr, the hardness slightly decreases to 71.3 HV but remains 15% higher than that of the base material.

The observed trends can be attributed to the following mechanisms:

(1) Strengthening Mechanism at Low Gr Content:

During RFE processing, frictional heat generated by the high-speed rotation of the stirring tool raises the matrix temperature to the critical value for dynamic recrystallization. Gr particles act as heterogeneous nucleation sites, promoting continuous dynamic recrystallization (CDRX) in the α-Mg matrix, leading to significant grain refinement (dominated by the Hall-Petch effect).

(2) Softening Mechanism at High Gr Content:

When the Gr content exceeds 1.5 wt.%, Gr particles form micron-sized agglomerates due to van der Waals forces. These agglomerates become stress concentration sources during plastic flow, and when their size exceeds a critical threshold, microcracks initiate, leading to a reduction in hardness. Additionally, the high thermal conductivity of Gr alters the thermal field distribution during RFE, resulting in incomplete local recrystallization and the formation of a mixed coarse/fine grain structure.

(3) Coupling Effect of Process-Structure-Properties:

The compatibility between extrusion rate and rotational speed determines the material's flow behavior. When the Gr content exceeds 1.5 wt.%, the increased flow resistance caused by Gr particles reduces the equivalent strain rate to the order of 10^2 s^{-1}, weakening the driving force for dynamic recrystallization.

In summary, the nonlinear variation in hardness of Gr/AZ31Mg composites is fundamentally a result of the combined influence of reinforcement content and process parameters on the microstructure. At Gr contents ≤ 0.5 wt.%, grain refinement and dispersion strengthening dominate. However, at Gr contents ≥ 1.5 wt.%, interface weakening and structural defects become the primary factors leading to performance degradation. This study provides a theoretical basis for optimizing the RFE process window and offers valuable insights for developing high-performance magnesium matrix composites.

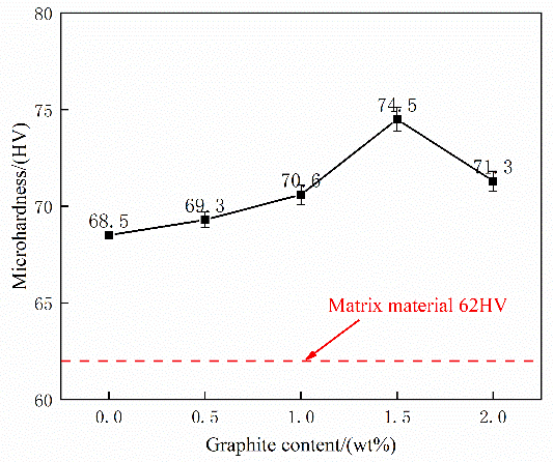

Figure 6. Relationship Between Composite Hardness and Graphite (Gr) Content

3.3. Friction and Wear Properties of Composites

Figure 7 presents the SEM images of the wear surfaces of composite materials. Figure 7(a) shows the wear surface of the RFE-state substrate specimen, where a certain degree of plastic deformation can be observed during the friction process. The surface exhibits the presence of an interface film, which contains some pits and a small number of plowing grooves. In the 1.5% Gr/AZ31Mg composite specimen, an interface film is also present; however, the surface appears smoother, with more numerous and deeper plowing grooves, while the number of pits gradually decreases. In contrast, the 2% Gr/AZ31Mg composite specimen exhibits an increased number of pits compared to Figure 7(b), and both the plowing grooves and pits are more densely distributed. This phenomenon may be attributed to the agglomeration effect of Gr particles at higher concentrations, which weakens the localized strengthening effect and consequently affects the overall wear resistance of the material.

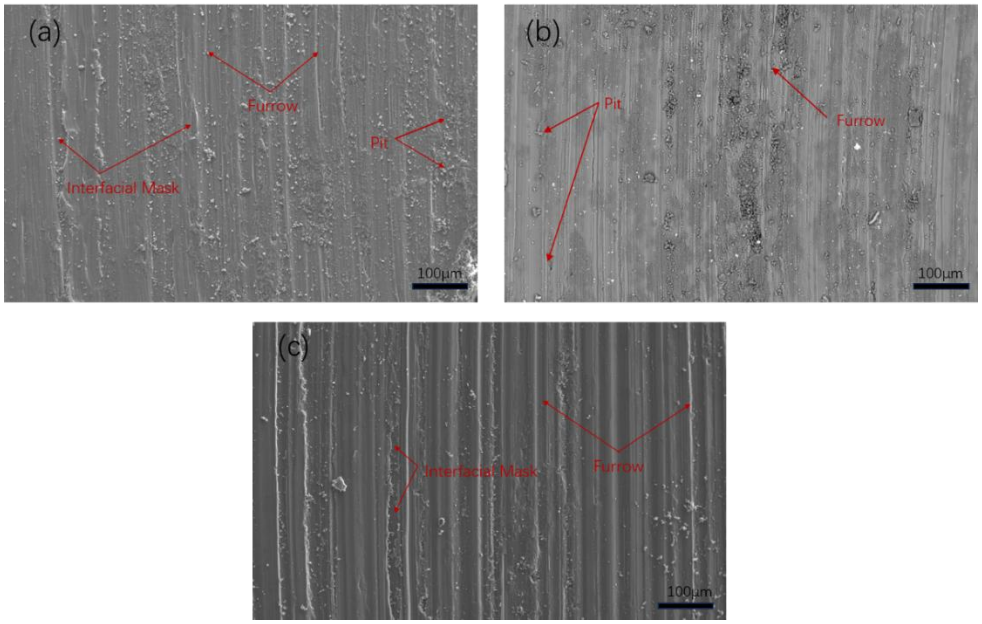

Figure 7. SEM images of the wear surfaces of the materials: (a) RFE-state substrate, (b) 1.5% Gr/AZ31Mg composite, (c) 2% Gr/AZ31Mg composite.

Figure 8 illustrates the relationship between the friction coefficient, wear rate, and Gr mass fraction in Gr/AZ31Mg composites. As shown in the figure, the RFE-state substrate exhibits the highest friction coefficient of 0.352. With the addition of Gr particles, the friction coefficient initially decreases and then increases. The minimum friction coefficient of 0.328 is observed at a Gr content of 1.5%, representing a 6.8% reduction compared to the RFE-state substrate. Additionally, the wear rate follows a similar trend to the friction coefficient. The RFE-state substrate exhibits the highest wear rate of 0.297, while the 1.5% Gr composite achieves the lowest wear rate of 0.197, marking a 33.7% reduction. When the Gr content increases to 2%, the wear rate rises slightly to 0.246, yet it still represents a 17.2% reduction compared to the RFE-state substrate.

The analysis indicates that the incorporation of Gr particles enhances the wear resistance of the composite material through multiple mechanisms. Firstly, the addition of Gr particles increases the hardness of the composite, thereby improving its resistance to plowing by the friction counterpart, effectively mitigating plastic deformation and wear during friction. Secondly, during the friction process, wear debris containing Gr particles gradually detaches and adheres to the contact surface between the composite and the friction counterpart, forming a uniform solid lubrication film. This lubrication film not only reduces the direct contact area between the matrix and the friction counterpart—concentrating frictional interactions between the friction counterpart and the lubrication film—but also lowers the interfacial friction coefficient, thereby significantly reducing the wear rate.

However, the effect of the Gr mass fraction exhibits a threshold phenomenon. At low Gr concentrations, the wear debris contains relatively few Gr particles, leading to a lubrication film primarily composed of matrix wear debris, resulting in weaker solid lubrication effects and relatively significant frictional wear. As the Gr content increases, the composite hardness is further enhanced, and the Gr concentration in the lubrication film increases, strengthening the lubrication effect and significantly reducing the wear rate. Nevertheless, when the Gr mass fraction reaches a certain level, the solid lubrication film stabilizes, and further increases in Gr content have a limited effect on enhancing wear resistance, causing the wear rate to plateau. Therefore, optimizing the Gr particle content within a reasonable range can effectively improve the wear resistance of the composite while avoiding the saturation effect associated with excessive addition.

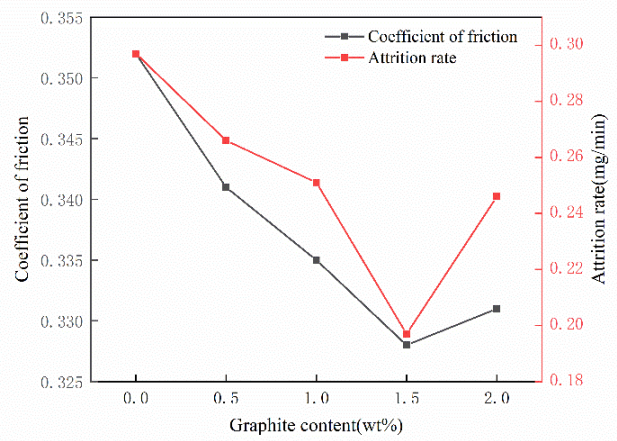

Figure 8. Relationship between the friction coefficient, wear rate, and Gr content in the composite material.

4. SUMMARY

The Gr/AZ31Mg composite prepared using the rotary friction extrusion (RFE) process exhibits excellent forming quality. Its microstructure is primarily composed of fine equiaxed grains formed through dynamic recrystallization, which contributes to improved mechanical properties and uniformity. Additionally, the Gr particles are uniformly distributed within the magnesium alloy matrix, effectively refining the microstructure and reducing local stress concentration, thereby enhancing the overall performance of the material.

Compared with the AZ31Mg alloy matrix without Gr particles, the Gr/AZ31Mg composite fabricated by the RFE process demonstrates higher microhardness. As the Gr mass fraction increases, the microhardness initially rises and then declines. The maximum microhardness of 74.5 HV is achieved at a Gr content of 1.5 wt%, representing a 20.2% improvement over the matrix material. This phenomenon can be attributed to the dispersion strengthening effect of Gr particles and their influence on the dynamic recrystallization process. However, when the Gr content continues to increase, particle agglomeration may lead to local stress concentration, causing a reduction in hardness.

During the wear process, Gr particles act as solid lubricants, reducing adhesion effects at the frictional contact interface, thereby decreasing wear volume and improving the wear resistance of the Gr/AZ31Mg composite. With increasing Gr content, both the friction coefficient and wear rate exhibit a downward trend. At a Gr mass fraction of 1.5%, the composite achieves the best wear resistance, with the lowest friction coefficient and wear rate. This optimal performance is likely due to the formation of a stable lubrication film at the friction interface, as well as the enhancement of the matrix's resistance to plastic deformation, effectively mitigating the wear process.

REFERENCES

[1] Suhuddin, U.F.H.R.; Mironov, S.; Sato, Y.S.; Kokawa, H.; Lee, C.W. Grain structure evolution during friction-stir welding of AZ31 magnesium alloy. Acta Mater. 2009, 57, 5406–5418.

[2] Tang, S.L.; Gao, Y.M.; Li, Y.F. Recent developments in fabrication of ceramic particle reinforced iron matrix wear resistant surface composite using infiltration casting technology. Ironmak. Steelmak. 2014, 41, 633–640.

[3] Fan, K.; Wang, G.Z.; Xuan, F.Z.; Tu, S.T. Effects of work hardening mismatch on fracture resistance behavior of bi-material interface regions. Mater. Des. 2015, 68, 186–194.

[4] Chen, W.; Yu, W.; Zhang, P.; Pi, X.; Ma, C.; Ma, G.; Zhang, L. Fabrication and performance of 3D co-continuous magnesium composites reinforced with Ti2AlNx MAX phase. Int. J. Miner. Metall. Mater. 2022, 29, 1406–1412.

[5] Wang, Z.; Nie, K.; Deng, K.; Han, J. Effect of extrusion on the microstructure and mechanical properties of a low-alloyed Mg−2Zn−0.8Sr−0.2Ca matrix composite reinforced by TiC nano-particles. Int. J. Miner. Metall. Mater. 2022, 29, 1981–1990.

[6] Mirzadeh, H. Surface metal-matrix composites based on AZ91 magnesium alloy via friction stir processing: A review. Int. J. Miner. Metall. Mater. 2023, 30, 1278–1296.

[7] Qian, X.; Yang, H.; Hu, C.; Zeng, Y.; Huang, Y.; Shang, X.; Wan, Y.; Jiang, B.; Feng, Q. Effect of potential difference between nano-Al2O3 whisker and Mg matrix on the dispersion of Mg composites. Int. J. Miner. Metall. Mater. 2023, 30, 104–111.

[8] Guan, H.; Xiao, H.; Ouyang, S.; Tang, A.; Chen, X.; Tan, J.; Feng, B.; She, J.; Zheng, K.; Pan, F. A review of the design, processes, and properties of Mg-based composites. Nanotechnol. Rev. 2022, 11, 712–730.

[9] Wang, B.-J.; Xu, D.-K.; Wang, S.; Xu, X.-B.; Han, E.-H. Effect of phosphate conversion film on fatigue and corrosion fatigue behavior of an as-rolled Mg–3.08Zn–0.83Al (in wt.%) alloy. J. Iron Steel Res. Int. 2023, 30, 2557–2565.

[10] Saikrishna, N.; Reddy, G.P.K.; Munirathinam, B.; Dumpala, R.; Jagannatham, M.; Sunil, B.R. An investigation on the hardness and corrosion behavior of MWCNT/Mg composites and grain refined Mg. J. Magnes. Alloys 2018, 6, 83–89.

[11] Kandemir, S.; Gavras, S.; Dieringa, H. High temperature tensile, compression and creep behavior of recycled short carbon fibre reinforced AZ91 magnesium alloy fabricated by a high shearing dispersion technique. J. Magnes. Alloys 2021, 9, 1753–1767.

[12] Meng, L.; Hu, X.; Wang, X.; Zhang, C.; Shi, H.; Xiang, Y.; Liu, N.; Wu, K. Graphene nanoplatelets reinforced Mg matrix composite with enhanced mechanical properties by structure construction. Mater. Sci. Eng. A 2018, 733, 414–418.